Adaptive Control Strategies for Flexible Space Structures

ANURADHA M. ANNASWAMY, Member, IEEE
Massachusetts Institute of Technology

DANIEL J. CLANCY
The Ohio State University

The problem of controlling flexible space structures in the presence of significant uncertainties using only position measurements is considered. Adaptive controllers, which are capable of controlling partially known dynamical systems and delivering good performance by providing a time-varying compensation on-line, are desirable for such systems. We present an adaptive controller which can globally stabilize a class of flexible structures. This controller is applicable whether position measurements, rate measurements, or combinations thereof are available, as well as for colocated and noncolocated actuator-sensor pairs that are sufficiently close. The improvement in performance generated using such controllers is demonstrated using two practical structural systems.

Manuscript received March 30, 1994; revised March 20, 1995.

IEEE Log No. T-AES/32/3/05868.

This work was supported by NSF Grant ECS 9296073.

Authors' addresses: A. M. Annaswamy, Dept. of Mechanical Engineering, Massachusetts Institute of Technology, 77 Massachusetts Ave., Rm. 3-461B, Cambridge, MA 02139; D. J. Clancy, Dept. of Electrical Engineering, The Ohio State University, 205 Dreese Laboratory, 2015 Neil Ave., Columbus, OH 43210.

I. INTRODUCTION

It is well known that the control of flexible space structures is a difficult task [1–3], which is mainly due to the intrinsic dynamic characteristics of these structures such as low damping and the presence of several and often densely packed modal frequencies. The difficulty in controlling them is exacerbated because of uncertainties present, which may be due to structural modifications, failure of system components, or changes in the operating environment. In the context of space structures, significant differences may exist between the dynamics exhibited by structures during on-ground tests and when deployed in space. Hence, control designs based on identification models which are typically derived using ground-based measurements are often highly sensitive to inaccuracies in the design model parameters and especially elastic modal frequencies. As pointed out in [4], even for a 1% error in the dominant mode frequency, the modeling error could be as large as the contribution of the mode itself. In addition, active control methods based on finite-dimensional techniques invariably lead to errors in both modal frequencies and mode shapes [5]. Not only does this introduce uncertainties in the modal frequencies and the modal shapes but also since different modes may be excited during different operating conditions, the total number of dominant modes in any given problem may also be unknown. For all of these reasons, an *adaptive controller*, which can function adequately in the presence of parametric uncertainties and deliver the required performance, is of considerable interest and importance for the control of flexible space structures.

The field of adaptive control has evolved over the past thirty years and grew out of attempts to control systems that are partially known. A significant part of this field has addressed dynamic systems that have parametric uncertainties. The adaptive control of linear time-invariant plants with unknown transfer functions has been studied at length and is currently well understood [6]. A key requirement for its implementation is that the order of the plant must be known. In addition, the stabilizing controller is correspondingly complex with an order twice as large as that of the plant. Requiring that the order of the system be known is quite a restrictive condition, especially in the context of flexible structures. Even if this number is known, it tends to be quite large, and as a result, it is not feasible to implement the requisite controller.

Linear time-invariant plants have been shown to be adaptively controllable if the order, the relative degree, and the sign of the high frequency gain of the underlying plant transfer function are known, and if the plant zeros are in $\mathbb{C}^-$. The relaxation of these assumptions has been attempted by several researchers (for example, [7, 8], where the focus was in determining if the above assumptions were indeed necessary for adaptive stabilization. Of particular relevance is the work of Morse in [7] which addresses adaptive stabilization of plants with unknown order. However, it does not deal with robustness behavior in the presence of disturbances or control objectives such as vibration suppression or tracking, which are the desired goals in the context of flexible structures; neither the issues of complexity of the requisite controller nor the resulting performance in specific examples are addressed.

Adaptive control of flexible structures has been considered elsewhere in [9–11]. The approach that has been used in these papers is based on what is termed as the *Command Generator Tracking* (CGT) method [12, 13]. For adaptive control based on the CGT method to result in global stability, several assumptions have to be satisfied [14]. Of these, the most restrictive one is that the outputs used for feedback must include rate measurements. In almost all test beds used for emulating the performance of large and complex flexible space structures, such as the ASCIE [15], the Large Spacecraft Control Laboratory (LSCL) [16], and a solar optical telescope model developed by CSDL [17], position information is readily available. If the underlying algorithm must use rate measurements thereby leading to differentiation of position data, it obviously leads to spikes in the presence of noise. Also, if rigid body modes are present, pure velocity feedback leads to unstable pole-zero cancellations. In [10], this difficulty was avoided by adding an inner loop control gain matrix to alter the modal characteristics of the plant and to convert the rigid body modes into finite frequency modes. However, since there can be destabilizing interactions between rigid body modes and the flexible modes of a structural system, this matrix cannot be implemented without having accurate knowledge of the plant.

In this work, we consider a class of flexible structures whose mode shapes, modal frequencies, and number of dominant modes are unknown. We present a new adaptive controller which is simple and of low order and requires no knowledge of the order of the underlying dynamic model. Using this controller, we establish that stable adaptive control can be realized using only position measurements in flexible structures. Whether on ground, or in space, it enables a strain-based sensing approach and allows the use of piezo-electric materials as active members for control actuation and displacement sensing [18, 19]. Using this controller, vibration suppression and shape controller are shown to result. We show that these objectives are realizable even when rigid body modes are present which makes the approach especially suitable for flexible structures in space. Adaptive control strategies are also presented for the case when only rate measurements, or both velocity and position measurements are available. We establish that satisfactory performance can be achieved not only with colocated actuator-sensor pairs, but also with a class of noncolocated actuator-sensor pairs that are sufficiently close.

The paper is organized as follows. In Section II, we discuss the underlying dynamics of a flexible space structure. We consider a linear finite-dimensional model, whose parameters correspond to the modal frequencies and the mode shapes. We then derive the input-output representations of the flexible structure, and discuss the relation between the dynamic models and the locations as well as types of actuators and sensors. In Section III, we show that vibration suppression and shape control can be established using the new controller when position measurements, rate measurements, or a combination of both, are available. Finally, in Section IV, the performance of these controllers is evaluated in two applications, an experimental control facility at Jet Propulsion Laboratory (JPL) [16], which has 30 modes whose frequencies lie between 0.1 and 5 Hz, and a flexible space station with 2 rigid body modes and 4 flexible modes [10], using simulation studies.

II. DYNAMIC MODEL

For a flexible space structure with small displacements, the linear dynamic equations describing the system are given by [3]

$$\begin{aligned} \ddot{r} + \mathrm{diag}(2\zeta_i\omega_i)\dot{r} + \mathrm{diag}(\omega_i^2)r &= B_a u + B_d \nu \\ y &= \begin{bmatrix} H_p & 0 \\ \alpha H_c & H_c \\ 0 & H_v \end{bmatrix} \begin{bmatrix} r \\ \dot{r} \end{bmatrix} \end{aligned} \tag{1}$$

where r is the vector of n modal coordinates, and ω_i and ζ_i are the natural frequency and damping ratio of the ith mode, respectively. $u \in \mathbb{R}^{n_a}$ is a vector of actuator inputs, $\nu \in \mathbb{R}^{n_d}$ is a vector of external disturbances, and $y \in \mathbb{R}^{n_p+n_c+n_v}$ is a vector of position, velocity plus scaled position, and velocity sensor outputs. The input matrices are given by $B_a = [b_1,\ldots,b_n]^{\mathrm{T}}$, $B_d = [d_1,\ldots,d_n]^{\mathrm{T}}$, where $b_i \in \mathbb{R}^{n_a}$, $d_i \in \mathbb{R}^{n_d}$, $i = 1,\ldots,n$, are the mode shapes evaluated at the n_a actuator locations, and n_d disturbance locations, respectively. The output matrices are defined as $H_p = [h_{p1},\ldots,h_{pn}]$, $H_c = [h_{c1},\ldots,h_{cn}]$, $H_v = [h_{v1},\ldots,h_{vn}]$ where $h_{pi} \in \mathbb{R}^{n_p}$, $h_{ci} \in \mathbb{R}^{n_c}$, $h_{vi} \in \mathbb{R}^{n_v}$, $i = 1,\ldots,n$, are the mode shapes at the n_p position sensor locations, n_c position + velocity sensor locations with $\alpha > 0$ as the scaling factor, and n_v velocity sensor locations, respectively. It is assumed that the system parameters in (1) as well as the number of modes n are unknown, and that an arbitrarily small but non-zero amount of modal damping ζ_i is present.

Depending on the number, the locations, and the types of actuators and sensors used, numerous input-output representations of the system in (1) can be derived. For instance, if the actuators and sensors are colocated,[1] it follows that

$$h_{xi} = b_i \qquad \forall \quad i = 1,\ldots,n \tag{2}$$

where the subscript $x = p$, c, or v, depends on whether position, scaled position + velocity, or velocity measurements are used. On the other hand, if the actuators and sensors are noncolocated but sufficiently close, the mode shapes at these different locations are similar. In such a case, the relation

$$\begin{aligned} h_{xi} &= (k + \epsilon_i) b_i \qquad \text{where} \\ k + \epsilon_i &> 0 \qquad \forall \quad i = 1,\ldots,n \end{aligned} \tag{3}$$

may be satisfied. In such a case, i.e., if the locations are such that (3) is satisfied, we define the actuators and sensors to be *proximally located*. The results developed here are applicable for both colocated and proximally located actuator-sensor pairs. We now derive the underlying input-output representations and their properties.

A single-input single-output (SISO) model: Assuming that there is a single actuator-sensor pair $\{u, y\}$, and a scalar disturbance ν at the actuator location, and n_c modes are controllable and observable, the input-output representation of the model in (1) is given by

$$y(t) = W_p(s)u(t) + W_d(s)\nu(t). \tag{4}$$

Throughout this work, the variable s is used to denote the differentiation operator d/dt. Lemma 1 is useful in determining the properties of $W_p(s)$ and $W_d(s)$.

LEMMA 1 *Let*

$$W(s) = \sum_{i=1}^{n} \frac{K_i}{s^2 + 2\zeta_i \omega_i s + \omega_i^2} \triangleq \sum_{i=1}^{n} W_i(s) = K\frac{p(s)}{q(s)}$$

where K_i, ζ_i, and ω_i are positive for $i = 1,\ldots,n$. Then the zeros and poles of $W(s)$ are in $\mathbb{C}^-$, the open left half of the complex plane.

PROOF Let $\alpha < \min_i(2\zeta_i\omega_i)$, $i = 1,\ldots,n$. Then the transfer functions $(s+\alpha)W_i(s)$ are strictly positive real for all $i = 1,\ldots,n$. As a result,

$$W(s) = \sum_{i=1}^{n} (s+\alpha) W_i(s) \quad \text{is SPR.}$$

Hence, the zeros and poles of $(s+\alpha)W(s)$ are in $\mathbb{C}^-$, which in turn implies that $p(s)$ and $q(s)$ are Hurwitz polynomials.

[1]As in [20], by *colocated sensors and actuators*, we mean that sensors and actuators are placed not only at the same physical positions but also along or about the same axis.

Case 1. Position Measurements: When y corresponds to a position measurement, the transfer function $W_p(s)$ is given by

$$W_p(s) = \sum_{k=1}^{n_c} \frac{h_{pk} b_k}{s^2 + 2\zeta_k \omega_k s + \omega_k^2}. \tag{5}$$

We note that $W_p(s)$ is of order $n_c \le n$, and has relative degree (number of poles—number of zeros) two. From Lemma 1, it follows that the zeros of $W(s)$ are in $\mathbb{C}^-$. For both colocated as well as proximally located actuator-sensor pairs, from (2) and (3), it follows that the numerator gain $h_{pk} b_k > 0$ for all $k = 1,\ldots,n_c$. Hence, it follows that in both cases, all zeros of $W_p(s)$ are in $\mathbb{C}^-$.

Case 2. Scaled Position + Velocity Measurements: When y corresponds to a scaled position + velocity measurement, with a scale factor $\alpha > 0$, the transfer function $W_p(s)$ is given by

$$W_p(s) = \sum_{k=1}^{n_c} \frac{h_{ck} b_k (s+\alpha)}{s^2 + 2\zeta_k \omega_k s + \omega_k^2}.$$

Once again, $W_p(s)$ is of order n_c, but has a relative degree unity. As in Case 1, if the input-output pair is colocated or proximally located, we have that the numerator gain $h_{ck} b_k > 0$. Since $\alpha > 0$, the zeros of $W_p(s)$ are in $\mathbb{C}^-$.

Case 3. Velocity Measurements: When y corresponds to a velocity measurement, the transfer function $W_p(s)$ becomes

$$W_p(s) = \sum_{k=1}^{n_c} \frac{h_{vk} b_k s}{s^2 + 2\zeta_k \omega_k s + \omega_k^2}.$$

As in the previous case, $W_p(s)$ is of order n_c, and has relative degree unity. Even though $h_{vk} b_k > 0$ for colocated and proximally located pairs, this only implies that all but one of the zeros of $W_p(s)$ are in $\mathbb{C}^-$, with one zero at $s = 0$.

In all the three cases, the transfer function $W_d(s)$ between the disturbance and the output is given by

$$W_d(s) = \sum_{k=1}^{n_c} \frac{h_{xk} b_k p(s)}{s^2 + 2\zeta_k \omega_k s + \omega_k^2}$$

where the subscript $x = p$, c, or v, and $p(s) = 1$, $(s+\alpha)$, or s depends on whether position, scaled position + velocity, or velocity measurements are used. Therefore, the order and the relative degree of $W_d(s)$ are equal to those of $W_p(s)$.

When rigid body modes are present in the flexible structure, we can express the transfer function $W_p(s) = W_r(s) + W_f(s)$ where W_r and W_f represent the contributions due to rigid body modes and flexible modes, respectively, at the ith output. If a position sensor is used, then $W_r(s) = (K_r/s^2)$, and

$$W_f(s) = \sum_{k=1}^{n_c} \frac{h_{pk} b_k}{s^2 + 2\zeta_k \omega_k s + \omega_k^2} \triangleq K_f \frac{N_f(s)}{D_f(s)}.$$

Hence

$$W_p(s) = K_r \frac{D_f(s) + (K_f/K_r)s^2 N_f(s)}{s^2 D_f(s)}.$$

From case 1, it follows that $K_f > 0$, and $D_f(s)$ and $N_f(s)$ are polynomials with roots in $\mathbb{C}^-$, of degrees $2n$ and $2n-2$, respectively. This implies that an arbitrarily small constant $k > 0$ exists such that

$$\text{the zeros of } W_p(s) \text{ has roots in } \mathbb{C}^- \qquad \forall \quad \frac{K_f}{K_r} < k. \tag{6}$$

Thus, when a position-controlled dynamic system with rigid body modes satisfies (6), the underlying transfer function has relative degree two, with zeros in $\mathbb{C}^-$. A similar property can also be derived when scaled position + velocity sensors are used for a system containing rigid body modes. However, the use of velocity sensors in the presence of rigid body modes leads to undesirable pole-zero cancellations and, hence, is avoided. For a given flexible structure, the smallness of (K_f/K_r) depends on the sum total of the contributions from all flexible modes relative to that of the rigid body mode at the ith location. If this is small, which is the case for most flexible structures, the above discussion indicates that the underlying transfer function is minimum phase. For the class of flexible structures considered in this work, we assume that if rigid body modes are present, they satisfy (6).

REMARK 1 In all the above cases, except when the output corresponds to a pure velocity measurement, $W_p(s)$ is a minimum phase transfer function. This property follows since 1) each mode is assumed to have non-zero damping, 2) the numerator gain of the ith mode $h_{xi}b_i$ is positive, and 3) the contributions from any existing rigid body modes are relatively large. All flexible structures have a certain amount of passive damping which justifies 1). Colocated actuator-sensor pairs automatically satisfy 2), whereas noncolocated actuator-sensor pairs satisfy 3) provided that the pair is *proximally located*. This is quantified in (3). Theoretically, as the number of modeled modes for any system represented by two nonidentical actuator-sensor locations becomes sufficiently large, $W_p(s)$ can become nonminimum phase [21]. However, for a given number of modes, n_c, a finite non-zero number of noncolocated actuator-sensor locations can be found for which the input-output transfer functions retain the minimum phase property.

A decoupled model: An obvious extension to the SISO model in (4) is a decoupled model with m actuator-sensor pairs $\{u_i, y_i\}$, $i = 1, \ldots, m$, which include n_p position sensors, n_c scaled position + velocity sensors, and n_v velocity sensors, with $m = n_p + n_c + n_p$. This can be expressed as

$$y(t) = W_p(s)u(t) + W_d(s)\nu(t) \tag{7}$$

where $y(t) = [y_1, \ldots, y_m]^T$, $u(t) = [u_1, \ldots, u_m]^T$, and $\nu(t) = [\nu_1, \ldots, \nu_m]^T$ is a disturbance vector, and the locations of the actuators, sensors, and disturbances are such that

$$\begin{aligned} W_p(s) &= \mathrm{diag}(W_{pi}(s)), \\ W_d(s) &= \mathrm{diag}(W_{di}(s)). \end{aligned} \tag{8}$$

The transfer function $W_{pi}(s)$ of the ith subsystem between u_i and y_i therefore satisfies all the properties discussed in the SISO case depending on the type of sensor at the ith location, for all $i = 1, \ldots, m$. The same holds for $W_{di}(s)$ as well. Such a decoupled system can be achieved by choosing the m locations in such a way that the n_i modes present in each $W_{pi}(s)$ are controllable and observable only through the corresponding input-output pair $\{u_i, y_i\}$, i.e., the mode shapes at the m locations are orthogonal to each other.

In summary, the class of flexible structures that is considered in this work is of the form of (7), where $W_p(s)$ and $W_d(s)$ satisfy (8) and the following properties hold.

P1) The order $n_i \le n$.

P2) The relative degree of $W_{pi}(s)$ is equal to one for colocated as well as proximally located actuator-sensor pairs with either a pure velocity measurement, or a velocity+ scaled position measurement.

P3) The relative degree of $W_{pi}(s)$ is equal to two for both colocated and proximally located pairs when the output measurement corresponds to a pure position measurement.

P4) In cases 1 and 2, all zeros are in $\mathbb{C}^-$; in case 3, one zero is at $s = 0$ and the remaining are in $\mathbb{C}^-$.

P5) If a rigid body mode is present, it is assumed that its contribution is large relative to those of the flexible modes, i.e., (6) is satisfied.

P6) If a disturbance is present, the relative degree of $(W_{di}(s)) \ge$ relative degree of $(W_{pi}(s))$.

Statement of the problem: With the model of the flexible structure given by (7) and (8), the problem is to design a control input u such that when a disturbance ν is present, or if there is an initial deflection on the structure, the displacements at various points on the structure settle down to zero as quickly as possible, i.e., $\lim_{t\to\infty} y(t) = 0$.

We also consider the problem of static shape control where it is required that the position response at different points on the structure are displaced by a finite amount [22]. As discussed in Section IV, this problem can be posed so that the output y follows a desired trajectory y_m, where the latter is specified as the solution of a homogeneous differential equation

$$\dot{x}_m = A_m x_m \qquad y_m = H_m^T x_m$$

where A_m is any stable matrix in $\mathbb{R}^{n_m \times n_m}$. For simplicity, we assume that A_m has a block diagonal structure so that

$$\dot{x}_{m_i} = A_{m_i} x_{m_i} \qquad y_{m_i} = h_{m_i}^T x_{m_i}$$
$$x_m = [x_{m_1}, \ldots, x_{m_{n_m}}]^T, \qquad y_m = [y_{m_1}, \ldots, y_{m_m}]^T \tag{9}$$

where A_{m_i} are stable matrices in $\mathbb{R}^{n_{m_i} \times n_{m_i}}$, $i = 1, \ldots, m$. If the output error is defined as e_1, where $e_1 = y - y_m$, our aim is to choose the control input u so that $\lim_{t\to\infty} e_1(t) = 0$.

III. ADAPTIVE CONTROL STRATEGIES FOR A FLEXIBLE STRUCTURE

In Section II, the dynamic models that describe the behavior of a flexible structure were discussed at length. It was seen that these structures have high order, low damping, unknown modal frequencies and/or modal shapes, and even an indeterminate number of dominant modes. The control of these structures has to therefore be carried out in the presence of such uncertainties. We develop a new adaptive controller and show that it leads to vibration suppression and shape control. In each case, we show that satisfactory control is achievable whether 1) only position measurements are available, 2) a combination of position and velocity measurements are available, or 3) only velocity measurements are available. Also, we show that these objectives are attainable using colocated as well as proximally located actuator-sensor pairs.

A. Vibration Suppression

In Section II, it was shown that the input-output representation can be expressed as

$$y = W_p(s)u + W_d(s)\nu \tag{7}$$

where $y, u, \nu : \mathbb{R}^+ \to \mathbb{R}^m$, and that the locations of the m actuator-sensor pairs can be chosen in such a way that the transfer matrices $W_p(s)$ and $W_d(s)$ are diagonal. It was also seen in Section II that each diagonal entry $W_{pi}(s)$ satisfies properties P1–P5 for $i = 1, \ldots, m$. The control objective is to choose an input u in (7) so that the displacements in various locations on the structure settle down to zero as quickly as possible, even when $W_p(s)$ and $W_d(s)$ are unknown. In Theorem 1, we describe the adaptive controller which ensures global stability as well as vibration suppression in all the modes that can be controlled through the m actuators in (7). For ease of exposition, we choose $m = 1$. The exact nature of the controller structure for multiple actuator-sensor pairs is elaborated in the next section.

THEOREM 1 *Let a flexible structure be described by* (7) *which satisfies properties* P1–P5. 1) *If y corresponds to position measurements, the controller is of the form*

$$\begin{aligned}
&\dot{\omega}(t) = -z_c \omega(t) + u(t) \qquad z_c > 0 \\
&u(t) = \theta_0(t) y(t) + p(t)\omega(t) - y(t)(\bar{y}^2(t) + \bar{\omega}^2(t)) \\
&\dot{\theta}_0(t) = -\gamma y(t)\bar{y}(t) \qquad \gamma > 0 \\
&\dot{p}(t) = -\gamma_p y(t)\bar{\omega}(t) \qquad \gamma_p > 0 \\
&\bar{y}(t) = (W_a(s))y(t) \qquad \bar{\omega}(t) = (W_a(s))\omega(t) \\
&W_a(s) = \frac{1}{s+a} \qquad a > 0.
\end{aligned} \tag{10}$$

2) *If y corresponds to either velocity, or velocity+ scaled position measurements, the controller is chosen as*

$$\begin{aligned}
&u(t) = \theta_0(t) y(t) \\
&\dot{\theta}_0(t) = -\gamma y^2(t) \qquad \gamma > 0.
\end{aligned} \tag{11}$$

In both cases, global boundedness of all signals follows and $\lim_{t\to\infty} y(t) = 0$.

PROOF *Case 1 Position Measurements*: The input-output relation for each component in (7) can be expressed as

$$y = W_p(s)u + W_d(s)\nu. \tag{12}$$

Properties P1–P5 imply that each diagonal entry $W_p(s)$ has relative degree two, minimum phase, with a positive high frequency gain. We show below that the controller in (10) leads to global boundedness in two steps.

Step 1 Let the disturbance $\nu \equiv 0$. We establish the existence of a stabilizing control input u of the form

$$\begin{aligned}
&u(t) = (z_c - p_c)\omega_1(t) + \theta_{0c} y(t) + r(t) \\
&\dot{\omega}_1(t) = -z_c \omega_1(t) + u(t) \qquad z_c > 0
\end{aligned} \tag{13}$$

where z_c, p_c, and θ_{0c} are constants. Equation (13) can also be written as

$$u = \left(\frac{s + z_c}{s + p_c}\right)[\theta_{0c} y + r].$$

The plant output y then becomes $y(t) = \overline{W}_m(s) r(t)$ where

$$\overline{W}_m(s) = \frac{kZ(s)(s + z_c)}{R(s)(s + p_c) + k\theta_{0c}(s + z_c)Z(s)}.$$

Let p_c^* be defined as

$$p_c^* = z_c + \sum_{k=1}^{n}(p_k) - \sum_{j=1}^{n-2}(z_j) + \delta \tag{14}$$

where δ is any arbitrary positive constant, and p_k and z_j are the real parts of the kth pole and the jth zero of $W_p(s)$, respectively. The poles of $\overline{W}_m(s)$ for different values of θ_{0c} can be determined by studying the root-locus of

$$\overline{W}_{mo}(s) = \theta_{0c} \frac{k(s + z_c)Z(s)}{(s + p_c)R(s)}. \tag{15}$$

Since $\overline{W}_{mo}(s)$ has relative degree two, there are two asymptotes with a centroid σ_A given by

$$\sigma_A = \frac{-p_c + \sum_k(p_k) - \sum_j(z_j) + z_c}{2}.$$

From (14), it follows that $\sigma_A > 0\ \forall p_c \geq p_c^*$. Therefore, a scalar θ_0^* exists such that $\forall\theta_{0c} \geq \theta_0^*$ and $\forall p_c \geq p_c^*$, $(n-1)$ poles of $\overline{W}_m(s)$ become arbitrarily close to its $(n-1)$ zeros, while the remaining 2 poles approach the asymptotes and hence have a real part $\sim -(\delta/2)$. Hence, when $r(t) \equiv 0$, the control input in (13) stabilizes the plant in (7).

Step 2 With a disturbance ν present, we choose the control input as in (13) but with time-varying parameters as

$$\begin{aligned} u(t) &= \theta_0(t)y(t) + p(t)\omega_1(t) \\ \dot{\omega}_1 &= -z_c\omega_1(t) + u(t), \qquad z_c > 0. \end{aligned} \tag{16}$$

Defining $\theta(t) = [\theta_0(t), p(t)]^T$, $\phi(t) = [\theta_0(t) - \theta_0^*, p(t) - p^*]^T$, and $\omega(t) = [y(t), \omega_1(t)]^T$ the closed-loop system can be expressed as

$$y(t) = \overline{W}_m(s)[\phi^T(t)\omega(t) + \nu(t)].$$

Since $\overline{W}_m(s)$ is of relative degree two, it cannot be shown to be strictly positive real. In order to generate a stable adaptive law, an additional signal $\dot{\theta}^T\overline{\omega}$ has to be added to the control input as [6, Sect. 5.4.3]

$$u(t) = \theta^T\omega(t) + \dot{\theta}^T\overline{\omega}(t) \tag{17}$$

where $\overline{\omega} = [1/(s+a)]\omega$. Equation (17) can be simplified further as

$$u = \theta^T(\dot{\overline{\omega}} + a\overline{\omega}) + \dot{\theta}^T\overline{\omega} = [s+a](\theta^T\overline{\omega}) \tag{18}$$

since $s = d/dt$, the differential operator. Equation (18) has the following two important implications.

1) When $\theta(t) \equiv \theta^* \stackrel{\Delta}{=} [\theta_0^*, p^*]^T$,

$$u(t) = [s+a](\theta^{*T})\left[\frac{1}{s+a}\right]\omega(t) = \theta^{*T}\omega(t)$$

which implies that the results of step 1 are unaffected.

2) With u as in (17), the plant output is given by

$$y = W_p(s)[\theta^T\omega + \dot{\theta}^T\overline{\omega} + \nu].$$

Since y decays exponentially to zero when $\theta = \theta^*$, we obtain that

$$y = \overline{W}(s)[\phi^T\omega + \dot{\phi}^T\overline{\omega} + \nu]$$

neglecting exponentially decaying initial conditions. Using (18), we obtain that

$$y = W_m(s)(\phi^T\overline{\omega} + \overline{\nu}) \tag{19}$$

where $\overline{\nu}(t) = [1/(s+a)]\nu(t)$ and $W_m(s) = \overline{W}_m(s)(s+a)$. Since $\nu \in \mathcal{L}^2$, $\overline{\nu} \in \mathcal{L}^2$. By the choice of a and $\overline{W}_m(s)$, $W_m(s)$ is SPR. From the results of Lemma 2, it follows that if the parameter error ϕ is adjusted as

$$\dot{\phi} = -\Gamma y\overline{\omega} \qquad \Gamma = \Gamma^T > 0$$

and we have the result that

$$y(t) \text{ and } \phi(t) \text{ are bounded} \qquad \forall \quad t \geq t_0, \quad \text{and} \quad y \in \mathcal{L}^2.$$

Since the state variables corresponding to $W_m(s)$ are bounded and since the signal in the reference model corresponding to ω_1 is bounded, it follows that $\omega_1 \in \mathcal{L}^\infty$. Therefore,

$$\lim_{t\to\infty} y(t) = 0 \qquad \text{if} \quad \nu \in \mathcal{L}^2 \cap \mathcal{L}^\infty$$

which proves Case 1.

Case 2 Velocity+ Scaled Position Measurements: In this case, since the output is proportional not only to position but also velocity, it follows that $W_p(s)$ has relative degree unity, while all the other assumptions remain the same as in case 1. Hence, a control input of the form

$$u(t) = \theta_{0c}y(t)$$

results in a closed-loop transfer function $W_m(s)$ which is asymptotically stable, minimum-phase, and has relative degree unity. Using root-locus arguments as above, it can be easily shown that $W_m(s)$ is strictly positive real $\forall\theta_{0c} \geq \theta_0^*$. Proceeding in a manner similar to case 1, if the control input is of the form of

$$u(t) = \theta_0(t)y(t)$$

the closed-loop system can once again shown to be of the form of (19). The controller in (11) together with the results of Lemma 2 lead to the proof of case 2.

Case 3 Velocity Measurements: In contrast to both the above cases, when only velocity measurements are available, as mentioned in Section II, $W_p(s)$ has one zero at $s = 0$ while the remaining ones are in $\mathbb{C}^-$. As a result, if the controller in (11) is used, the underlying transfer function $W_m(s)$ can no longer be shown to be minimum phase. We therefore use a different approach to establish regulation.

The state-variable description can be expressed in the form [21]

$$\begin{aligned} \dot{x} &= Ax + bu + d\nu \\ y &= h^Tx \end{aligned}$$

where $A = \mathrm{diag}(A_j)$, $h = [h_1^T, \ldots, h_n^T]^T$, $b = [b_1^T, \ldots, b_n^T]^T$,

$$A_j = \begin{bmatrix} 0 & 1 \\ -\omega_j^2 & -2\zeta_j\omega_j \end{bmatrix},$$

$$b_j = \begin{bmatrix} 0 \\ \overline{b}_j \end{bmatrix},$$

$$h_j = \begin{bmatrix} 0 \\ \overline{h}_j \end{bmatrix}$$

and $\overline{b}_j$ and $\overline{h}_j$ are the system parameters corresponding to the jth mode. Expressing the control parameter $\theta_0(t) = \theta_0^* + \phi_0(t)$, the closed-loop system equations corresponding to the control input in (11) are given by

$$\begin{aligned} \dot{x} &= \overline{A}x + b(\phi^T \omega + \overline{\nu}) \\ y &= h^T x \end{aligned} \tag{20}$$

where $\overline{A} = \mathrm{diag}(\overline{A}_j)$, and

$$\overline{A}_j = \begin{bmatrix} 0 & 1 \\ -\omega_j^2 & -2\zeta_j\omega_j + \theta_0^*\overline{b}_j\overline{h}_j \end{bmatrix}.$$

Let $k = 2\theta_0^*$, and $M_0 = qq^T$, where $q = [q_1^T, \ldots, q_n^T]^T$, and $q_j = [0, 2\sqrt{\zeta_j\omega_j(c+\epsilon_j)}]^T$. Then a matrix P of the form $P = \mathrm{diag}(P_j)$ where

$$P_j = \begin{bmatrix} \omega_j^2(c+\epsilon_j) & 0 \\ 0 & (c+\epsilon_j) \end{bmatrix}$$

is the solution of

$$\begin{aligned} \overline{A}^T P + P\overline{A} &= -khh^T - M_0 \\ Pb &= h. \end{aligned}$$

Stability can be shown along very similar lines to that of Lemma 2 by considering a scalar positive-definite function $V(x,\phi)$ and showing that it is bounded, where x corresponds to the state variables of the closed-loop system.

The adaptive controller suggested in this work is applicable to the control of a class of flexible structures described by (7) which is a decoupled, linear, finite-dimensional multiple-input multiple-output (MIMO) model, with rigid body modes as well as flexible modes. As is seen in Theorem 1, the controller requires at most two adjustable parameters for vibration suppression, irrespective of the number of rigid body and flexible modes.

A special case: Often in many flexible structures, the damping characteristics are such that the poles and zeros of $W_p(s)$ satisfy the relation

$$\sum_k (p_k) - \sum_j (z_j) < 0 \tag{21}$$

where p_k and z_j are the real parts of the ith pole and the jth zero. For instance, when there is uniform modal damping, using simple extensions of the result in [18], it can be shown that

$$p_i < z_j < p_{i+1} \qquad \forall \quad i,j = 1,\ldots,n-1$$

which in turn implies (21). Similarly, when all modes have a uniform settling time, it follows that the real parts of the $(2n-2)$ zeros are identical to that of $2n-2$ poles which once again leads to the relation in (21). In such cases, the parameter $p(t)$ can be fixed as $p(t) \equiv p_c = z_c + \delta$, $\delta > 0$. This simplifies the control input in (10) as

$$u(t) = G_c(s)[\theta_0(t)y(t) - y(t)\overline{y}^2(t)] \tag{22}$$

where $G_c(s) = [(s+z_c)/(s+p_c)]$. Without loss of generality, the compensator $G_c(s)$ can be modified as

$$G_c(s) = k_c\left(\frac{s+z_c}{s+p_c}\right) \qquad k_c > 0.$$

In the examples discussed in Section IV, it is seen that such a control input leads to good performance with reasonable values of θ_0.

The controller in Theorem 1 can be modified to include a proportional adjustment. For instance, in case 2, the control input can be modified as

$$\begin{aligned} u(t) &= \overline{\theta}_0(t)y(t) \\ \overline{\theta}_0(t) &= \theta_{0p}(t) + \theta_0(t) \\ \theta_{0p}(t) &= -y^2(t) \end{aligned}$$

with θ_0 adjusted as in (11). A similar adjustment can be made for position measurements and velocity measurements as well. The proof of stability can be established in all cases along very similar lines to that in Theorem 1.

The global stability in Theorem 1 follows provided the disturbance $\nu \in \mathcal{L}^2$. If on the other hand, $\nu \in \mathcal{L}^\infty$, this result no longer holds. To ensure boundedness in such a case, modifications to the adaptive law have to be introduced [22, 23]. For instance, the adaptive laws in (11) in Theorem 1 have to be modified as

$$\dot{\theta}_0(t) = -\sigma\theta_0(t) - y^2(t), \qquad \sigma > 0$$

which can be shown to result in boundedness of all solutions. A similar modification to the adaptive laws in (10) will assure boundedness when $n^* = 2$ as well.

The main contribution of this work is that vibration suppression (and shape control, as shown in the next section) is possible in flexible structures using only position measurements. This is achieved by making explicit use of the fact that, in this case, the relative degree of the plant transfer function is two and the fact that colocated and proximally located actuator-sensor pairs yield zeros in $\mathbb{C}^-$. In the adaptive control literature, when $n^* = 2$, a stabilizing controller has been derived for SISO linear time-invariant plants [24]. However, the requisite controller requires the order of the plant to be known explicitly, unlike the one presented here. As mentioned in the introduction, relative degree information has been used in the past for stabilizing plants [7, 25]. But the robustness properties of such controllers and their performance in the context of a practical application have not been established heretofore. In contrast to these, we present a low-order controller, consider regulation and model-following in the context of flexible structures, and establish its robustness with respect to disturbances in $\mathcal{L}^2$ and $\mathcal{L}^\infty$. In the next section, we discuss two illustrative examples of space structures, their properties, the applicability of the proposed controller to their control, and the resulting simulation studies on their dynamic model. It should also be mentioned that in [26], this controller is also shown to be robust with respect to unmodeled dynamics that are sufficiently small.

The algorithm developed in Theorem 1 obviously is applicable to only decoupled models of flexible structures. When multiple actutator-sensor pairs are used, such an assumption requires that the mode shapes occurring at the actuator and sensor locations be orthogonal. Usually, this can be ascertained from the symmetries present in the structure. Also, in general, translational and rotational motion are often decoupled in structures [16, 27], resulting in orthogonal mode shapes. For instance, in the first example discussed in Section IV, it is shown that two separate locations can be determined on the structures for placing two colocated actuator-sensor pairs based on the geometry of the structure, leading to a 2×2 decoupled dynamic model. It is obvious that extensions to strongly coupled MIMO plants as well as to plants with arbitrary zeros need to be established to increase the scope the application of our algorithms. Our preliminary investigations indicate that the controller suggested here results in boundedness even for these extensions [28]. In fact, the examples discussed in Section IV illustrate that superior performance can be obtained using this controller not only for decoupled plants but also for strongly coupled MIMO plants.

B. Shape Control

We now consider the problem of shape control where it is required that the displacements at various points on the structure have to achieve certain steady-state values so as to obtain a static shape. The desired values for the various points can then be represented as y_m, the output of a homogeneous differential equation, as in (9). The problem is then posed as the choice of u in (7) so that y_p follows y_m asymptotically. With only a slight modification of the proof in Theorem 1, we show that an additional term $\theta_m^T x_m$ in the control input leads to trajectory following, where x_m is as defined in (9), and θ_m is a time-varying parameter that is adaptively adjusted. For ease of exposition, we assume that (21) is satisfied by the flexible structure.

THEOREM 2 *Let the dynamic model in* (7) *denote the input-output relation of a flexible structure, and* (9) *specify the desired response* y_m. *We define* $e = y - y_m$, $\theta = [\theta_0, \theta_m^T]^T$, *and* $\omega = [y(t), x_m^T(t)]^T$. 1) *If the output*

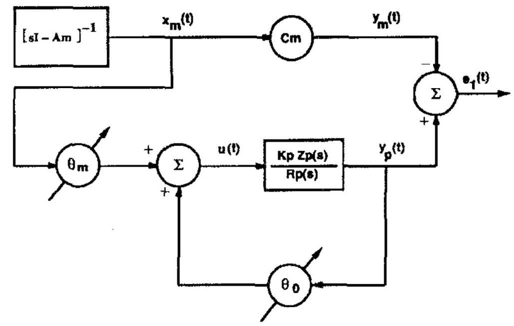

Fig. 1(a). New adaptive controller ($n^* = 1$).

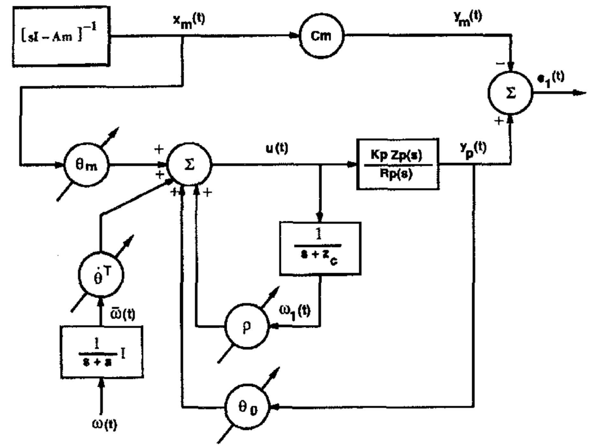

Fig. 1(b). New adaptive controller ($n^* = 2$).

corresponds to a position measurement, the control input u are chosen as [*Fig.* 1(b)]

$$
\begin{aligned}
u(t) &= G_c(s)[\theta^T(t)\omega(t) - e(t)\overline{\omega}^T(t)\overline{\omega}(t)] \\
\dot{\theta}(t) &= -\Gamma e(t)\overline{\omega}(t) \qquad \Gamma > 0 \\
\overline{\omega}(t) &= (W_a(s))\omega(t) \\
G_c(s) &= \operatorname{diag}\left(\frac{s + z_c}{s + p_c}\right), \\
W_a &= \operatorname{diag}\left(\frac{1}{s + a}\right) \\
0 < z_c < p_c & \qquad 0 < a < 2(p_c - z_c).
\end{aligned}
\tag{23}
$$

2) *If y corresponds to a* velocity+ scaled *position or a pure velocity measurement, the input is of the form* [*Fig.* 1(a)]

$$
\begin{aligned}
u(t) &= \theta^T(t)\omega(t) \\
\dot{\theta}(t) &= -\Gamma e(t)y(t) \qquad \Gamma > 0 \\
\dot{\theta}_m(t) &= -\Gamma_m e(t)x_m(t) \qquad \Gamma_m > 0.
\end{aligned}
\tag{24}
$$

In both cases, global boundedness of all signals follows, and $\lim_{t\to\infty} e(t) = 0$.

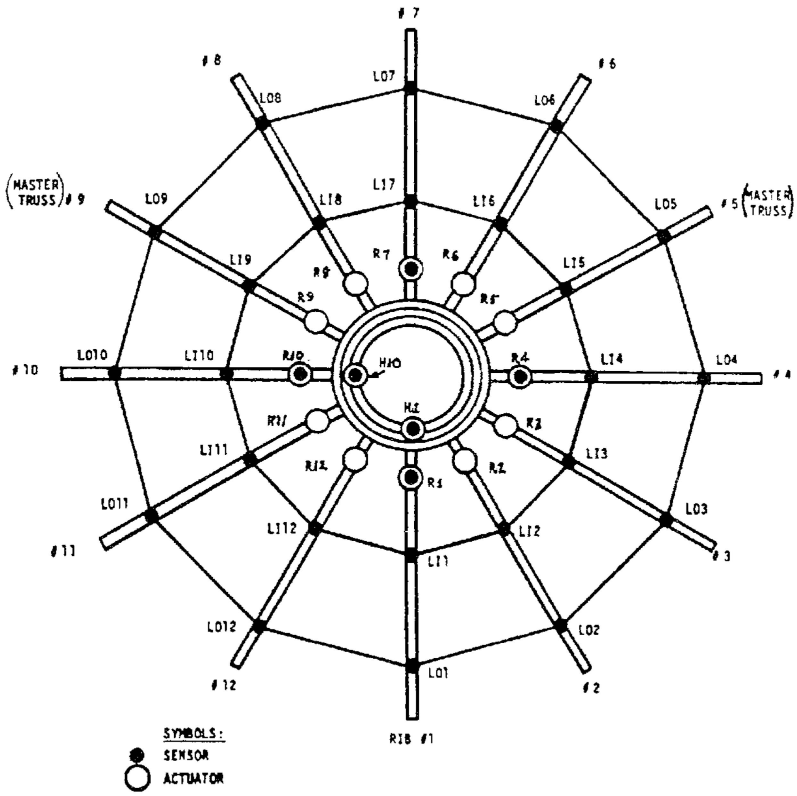

Fig. 2. Plan view of LSCL structure with actuators and sensors.

PROOF The results of Theorem 1 imply that when $y_m(t) \equiv 0$, then boundedness follows and $\lim_{t\to\infty} e(t) = 0$. The latter therefore has to be established when $y_m(t)$ satisfies (9). This is accomplished by the introduction of an additional term $\theta_m^T(t)x_m(t)$ in u and appropriate adjustment of $\theta_m(t)$. We show the proof below for case 2.

A constant θ_m^* exists such that if

$$u = \theta_0^* y + \theta_m^{*T} x_m \tag{25}$$

then $e(t)$ approaches zero asymptotically. This follows since the matrix corresponding to the closed-loop system is given by

$$S = \begin{bmatrix} A_p + b_p\theta_0^* h_p^T & b_p \\ h_p^T & 0 \end{bmatrix}$$

where $W_p(s) = h_p^T(sI - A_p)^{-1}b_p$, S is invertible, with transmission zeros in $\mathbb{C}^-$, from the results of [12, 13].

Replacing the constant parameters θ_0^* and θ_m^* in (25) by $\theta_0(t)$ and $\theta_m(t)$ and proceeding as in the proof of Theorem 1, it can be shown that the underlying error equation is of the form

$$e = W_m(s)[\phi^T\omega + \nu]$$

where $W_m(s)$ is the transfer function corresponding to S and is SPR. Therefore the adaptive laws in (24) and Lemma 2 lead to the proof of Theorem 2.

IV. ILLUSTRATIVE APPLICATIONS

The discussions in Sections II and III indicated that provided the flexible structure can be modeled using (7) and (8), the adaptive controllers delineated in Sections IIIA and IIIB ensure that vibration suppression and shape control are possible, respectively. In this section, we present two flexible structures and their performance using the adaptive controllers in Section IIIA. The first is an experimental facility called the Large Spacecraft Control Laboratory (LSCL) developed jointly by JPL and AFAL, which replicates the main properties of a flexible space structure that are most relevant when implementing active control methods. The second is a flexible space station with a two-panel configuration. In both cases, we discuss the dynamic model, choose the actuator-sensor locations, their number, and the type of sensors. We incorporate the new controller proposed in this work, and present the resulting system performance through simulation studies. In each case, we discuss whether the assumptions under which the proposed controller is stable are indeed satisfied by the structures.

1) *The LSCL* [16]: The structure is a large, 20 ft diam, 12 rib circular antenna-like flexible structure with a gimballed central hub and a long flexible feed-boom assembly (see Fig. 2 for a plan view of the structure with sensor and actuator locations). The ribs

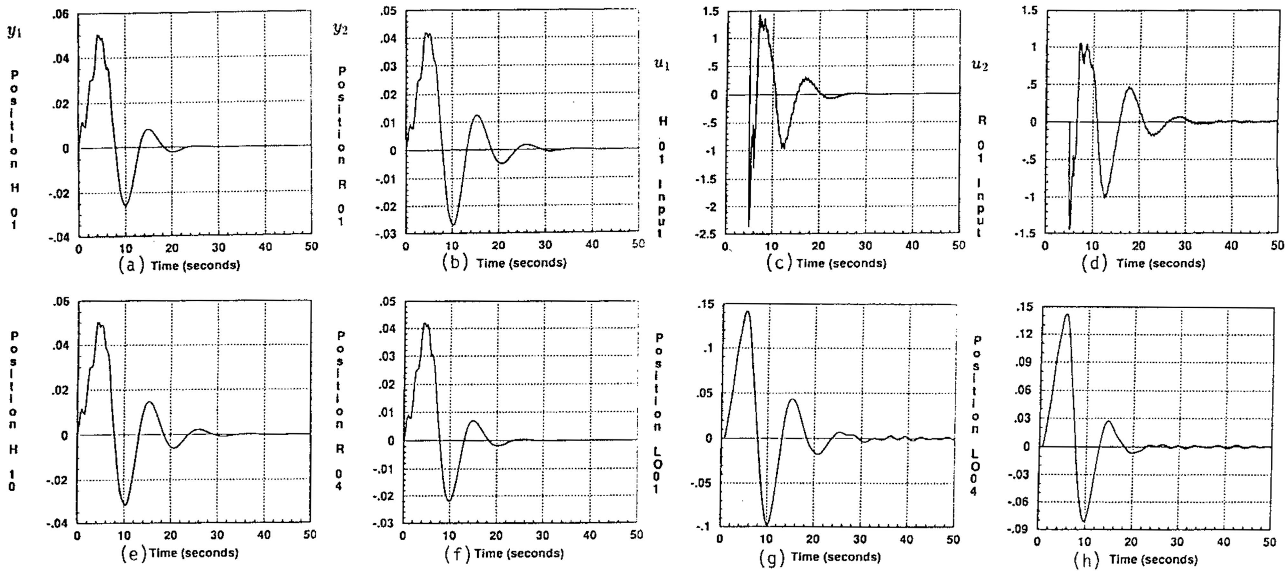

Fig. 3. Adaptive control for LSCL structure with two colocated actuator-sensor pairs using position feedback (refer to Fig. 2 for actuator-sensor locations).

are very flexible in the vertical, out-of-plane direction, and are coupled to one another by tensioned wires which dynamically simulate the coupling effect of a mesh on a real antenna. The input-output data was generated using a 10 degree-of-freedom finite-element model with 30 flexible modes and no rigid body modes and a uniform modal damping of 0.001. A total of 6 actuators can be placed at the locations H1, H10 (hub torquers), R1, R4, R7, and R10 (rib root torquers). Thirty sensors can be placed throughout the structure, including the 6 actuator locations and 24 locations on the 12 ribs. An actuator disturbance is introduced at the hub torquers. The control objectives are to minimize the displacements at various locations on the structure, while returning the structure to equilibrium as quickly as possible.

We present three simulations of the structure response using the controller in Section IIIA. For all the three simulations, *no knowledge* of the modal frequencies was used. In each case the number as well as the location of actuators and sensors were different. In the first case, this corresponded to 2 colocated actuator-sensor pairs. The locations H1 and R1 were chosen to place these two pairs since the former measures the rotational motion of the hub about the rib 1–7 axis while the latter measures the linear displacement of the rib at R1 and hence correspond to decoupled motions. Therefore the dynamic model of the structure is in the form of (7) and (8). Since our goal is vibration suppression, the algorithm presented in Section IIIA is relevant. The control input is realized according to (10) or (11) depending on whether the sensor output corresponds to position information or a linear combination of position and velocity. No other information regarding the actual mode shapes of the structure is needed to implement the controller. In the second simulation, we chose 4 actuator-sensor pairs at R1, R4, R7, and R10. At these locations, we do not have decoupled motions, and hence, (8) is no longer valid. However, the responses obtained (Fig. 4) give credence to our belief that the approach reported here can be extended to general multivariable systems that occur in flexible structures [28]. In the third simulation, we placed a colocated sensor-actuator pair at H1 and proximally located a second pair with a force-actuator at R1 and a position sensor at LI1. The resulting system is decoupled for the same reasons as for simulation 1. These three simulations are described in more detail below.

Simulation 1: We colocated two actuator-sensor pairs to generate the input-output measurements, one at H1, and the other at R1, with the sensor outputs corresponding to position measurements. Denoting the input-output variables at these locations as $\{u_i, y_i\}$, $i = 1,2$, a controller of the form

$$\left.\begin{aligned} u_i &= \left[\frac{s+0.1}{s+500}\right]\{\theta_{0i}y_i - y_i\overline{y}_i^2\} \\ \overline{y}_i &= \left[\frac{1}{s+500}\right]y_i \\ \dot{\theta}_{0i} &= -\gamma_{0_i}y_i\overline{y}_i \end{aligned}\right\} \quad i = 1,2 \qquad (26)$$

was implemented. All initial conditions were set to zero, and $\gamma_{0_1} = \gamma_{0_2} = 10^6$. The adaptive controller for all cases is turned on after 5 s. The resulting position responses as well as the actuator inputs at both H1 and R1 are indicated in Fig 3(a)–(d). Position responses at other locations (H10, R4, L01, L04) are included in Fig. 3(e)–(h). The units for the hub sensor responses (H1, H10), for the rib sensor responses (R1, R4, R7, R10, LI1–LI12, and LO1–LO12), and the actuator

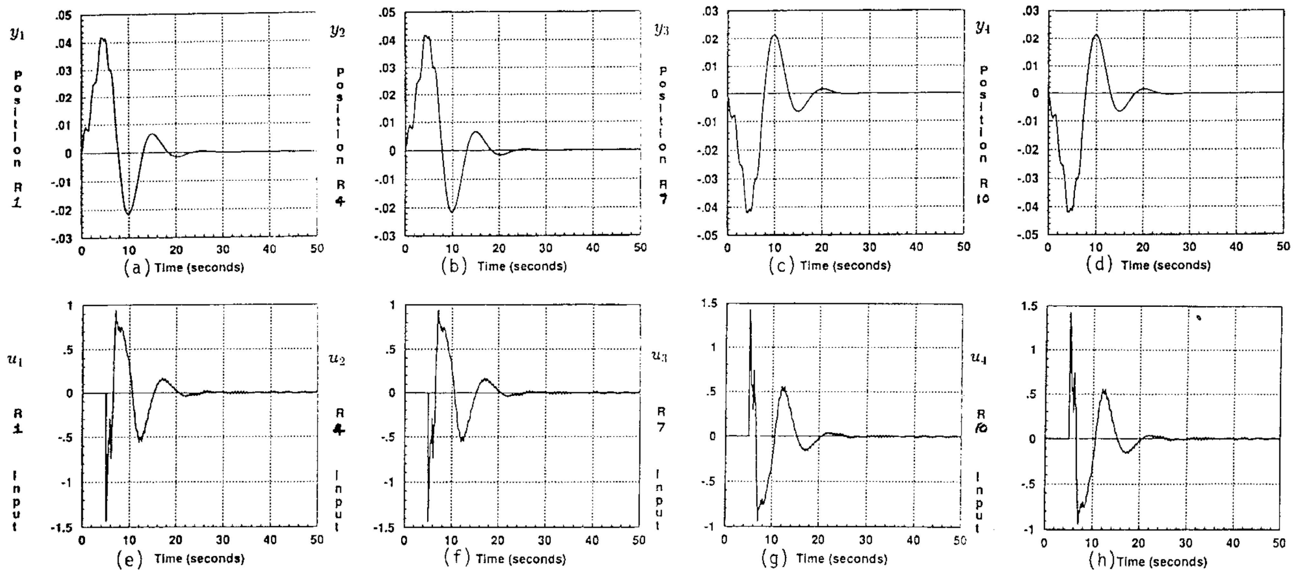

Fig. 4. Adaptive control for LSCL structure with four colocated actuator-sensor pairs using position feedback (refer to Fig. 2 for actuator-sensor locations).

inputs are in radians, meters, and Newton-meters, respectively. It is seen that the settling time is within 20 s with minimal overshoot.

Simulation 2: Next, we selected four locations R1, R4, R7, and R10, and we used a controller as in (26), for $i = 1,\ldots,4$, where $\{u_i, y_i\}$ correspond to force-input and position-output measurements at these locations. The responses using position sensors are presented in Fig. 4(a)–(h) and are seen to be satisfactory. The amplitudes of the actuator inputs and the steady-state feedback gains θ_1 and θ_2 were in fact slightly lower than those for case 1, since the burden of control was spread over 4 actuators, decreasing the requirements on any one actuator.

Simulation 3: We colocated one actuator-position sensor pair at H1 and proximally located a second pair with a force-actuator at R1 and a position-sensor at LI1 with the resulting 2×2 system being decoupled for the same reasons as described in experiment 1. With $\gamma_1 = 10^6$ and $\gamma_2 = 10^{12}$, a controller was implemented as in (26). The resulting responses were low in amplitude at H1 and LI1, but considerably larger at all other sensor locations affected by actuator R1. Similar observations were made when 4 proximally located actuator-position sensor pairs, R1–LI1, R4–LI4, R7–LI7, and R10–LI10, were used. This indicates that the theory developed in this work is applicable to noncolocated actuator-sensor pairs, but can stand further improvement.

2) *The Flexible Space Station* [10]: Various configurations have been developed by NASA for the proposed space station. One of them has a two-panel planar configuration, whose dynamic model consists of 2 rigid modes, and 4 flexible modes between 0.04 Hz and 0.3947 Hz with a uniform modal damping of 0.005. The problem is to determine a control strategy to contain the effect of initial condition deflections on angles β_1, β_2, and β_3, and position z_2. The initial conditions placed on the individual nodes of the space station were the same as those used in [10]. In addition to being strongly coupled, the underlying system also has rigid body modes. With the same adaptive controller structure as in (26), for $i = 1,\ldots,4$, the performance when position measurements were utilized are indicated in Fig. 5(a)–(d) and are seen to be satisfactory. As in the first application, here too it is seen that even though at these four locations, the modes are not decoupled, the controller as in (26) still leads to satisfactory performance. The presence of rigid body modes, which is a necessary feature in all space structures, does not affect the system performance.

V. CONCLUSIONS

In this paper, we considered a class of flexible structures whose mode shapes, modal frequencies, and number of dominant modes are unknown, and has a decoupled dynamic model. We presented a new adaptive controller which is simple and of low order, required no knowledge of the order of the underlying dynamic model or the modal frequencies, and led to vibration suppression as well as shape control using colocated and proximally located actuator-sensor pairs, even in the presence of rigid body modes. Two illustrative examples including a ground-based laboratory structure and a space station were presented to evaluate the adaptive controller proposed, which indicated that by using position measurements and colocation, the adaptive controller can be successfully deployed to get adequate performance. No knowledge of modal frequencies or

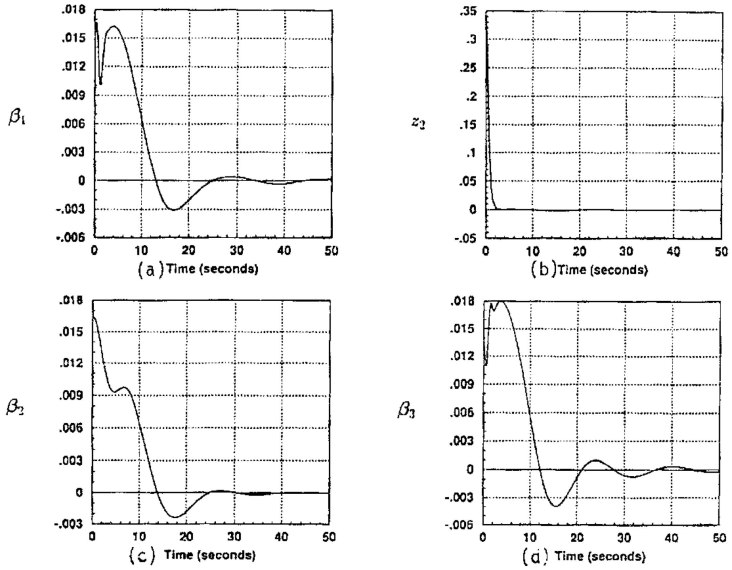

Fig. 5. Adaptive control for a space station, a strongly coupled MIMO flexible structure with four colocated actuator-sensor pairs using position feedback.

exact mode shapes was required to implement the controller. The same results can also be derived using either only velocity measurements, or velocity + scaled position measurements.

Complexities of large projects such as the Space Station Freedom demand that the attitude control systems should be such that stability and precise pointing performance is maintained for a large excursion in system parameters. Since the adaptive controller proposed here does not require any knowledge of the parameter values, it can accommodate typical uncertainties that may occur in space structures such as changes in the system parameters due to changes in moments of inertia or moving mass, or due to variations in stiffness. This makes the proposed controller especially attractive in applications where stability and precise pointing performance needs to be maintained in the presence of large variations in the system parameters.

ACKNOWLEDGMENTS

We would also like to thank Dr. Asif Ahmed at JPL for providing us with the data for the LSCL structure.

APPENDIX A

LEMMA 2 *Let $\phi(t)$, $\omega(t)$ be vectors in $\mathbb{R}^n$, and $e_1(t)$ be a scalar variable, where e_1 and ω can be measured at every instant of time, while ϕ is unknown but can be adjusted at every instant. If the underlying system is given by*

$$e_1(t) = W(s)[\phi^T(t)\omega(t) + \nu(t)] \tag{27}$$

where $\nu(t)$ is a scalar signal that arises due to disturbances, and $W(s)$ is a strictly positive real transfer function. If the parameter ϕ is adjusted according to the rule

$$\dot{\phi}(t) = -\Gamma\, e_1(t)\omega(t) \qquad \Gamma = \Gamma^T > 0. \tag{28}$$

If the disturbance has a finite energy,

$$\nu \in \mathcal{L}^2 \Rightarrow e_1(t) \quad \text{and} \quad \phi(t) \text{ are bounded}$$
$$\forall \quad t \geq t_0, \quad \text{and} \quad e_1 \in \mathcal{L}^2.$$

If, in addition, $\omega(t)$ and $\nu(t)$ are bounded, then

$$\lim_{t\to\infty} e(t) = 0, \qquad \lim_{t\to\infty} e_1(t) = 0.$$

PROOF Since $W(s)$ is strictly positive real, the Kalman–Yakubovich Lemma assures that a matrix $P = P^T > 0$ exists such that

$$A^T P + PA = -Q, \qquad Pb = h$$

where $W(s) = h^T(sI - A)^{-1}b$ and $Q = Q^T > 0$. Also, (27) can be expressed as

$$\dot{e} = Ae + b(\phi^T\omega + \nu) \qquad e_1 = h^T e.$$

To establish boundedness, we choose a positive-definite function $V(e, \phi)$ as

$$V = e^T Pe + \phi^T \Gamma^{-1} \phi$$

which leads to a time-derivative $\dot{V}$ to be

$$\dot{V} = -e^T Qe + 2e_1\nu. \tag{29}$$

When no disturbances are present, i.e., $\nu(t) \equiv 0$, then $\dot{V} \leq 0$, and hence, it immediately follows that $e_1(t)$ and $\phi(t)$ are bounded for all $t \geq t_0$. We also obtain that

$$\int_{t_0}^{\infty} \dot{V}(\tau)d\tau < \infty \Rightarrow e \in \mathcal{L}^2.$$

If $\omega(t)$ is bounded, then $\dot{e} \in \mathcal{L}^\infty$. Barbalat's Lemma [5] ensures that

$$e, \dot{e} \in \mathcal{L}^\infty, \qquad \text{and}$$
$$e \in \mathcal{L}^2 \Rightarrow \lim_{t\to\infty} e(t) = 0,$$
$$\lim_{t\to\infty} e_1(t) = 0.$$

When a disturbance ν is present, we cannot proceed as above, since $\dot{V}$ is no longer sign-definite. Boundedness can however still be established by considering the behavior of $V(t)$ over a time interval $[t_0, t]$. In what follows, c_i, $i = 1, \ldots, 8$, are finite positive constants. Integrating (29) on both sides from t_0 to t, we obtain that

$$\int_{t_0}^{t} \dot{V}(\tau)\, d\tau = \int_{t_0}^{t} -e^T Q e\, d\tau + 2\int_{t_0}^{t} e_1 \nu\, d\tau \qquad \text{or}$$

$$V(t) - V(t_0) \le -c_1 \int_{t_0}^{t} \|e\|^2 d\tau + 2c_2 \left[\int_{t_0}^{t} \|e\|^2 d\tau \int_{t_0}^{t} |\nu|^2 d\tau\right]^{1/2} \tag{30}$$

using Cauchy–Schwartz inequality. The state error e must satisfy either the condition that

$$\text{a) } e \in \mathcal{L}^2 \qquad \text{or} \qquad \text{b) } e \notin \mathcal{L}^2.$$

If $e \in \mathcal{L}^2$, then (30) can be simplified as

$$V(t) - V(t_0) \le 2c_3 \left[\int_{t_0}^{t} |\nu|^2 d\tau\right]^{1/2} \le 2c_3 c_4$$

since $\nu \in \mathcal{L}^2$. Therefore,

$$V(t) \le c_5 \qquad \forall \quad t \ge t_0$$

which implies that $e(t)$ and $\phi(t)$ are bounded for all $t \ge t_0$.

Let $e \notin \mathcal{L}^2$. Since (30) can be expressed as

$$V(t) - V(t_0) \le -c_1 \left[\int_{t_0}^{t} \|e\|^2 d\tau\right]^{1/2} \times \left\{ \left[\int_{t_0}^{t} \|e\|^2 d\tau\right]^{1/2} - \frac{2c_2}{c_1} \left[\int_{t_0}^{t} |\nu|^2 d\tau\right]^{1/2} \right\} \tag{31}$$

when $e \notin \mathcal{L}^2$, for some t_1 and $\forall t \ge t_1$,

$$\int_{t_0}^{t} \|e\|^2 d\tau \ge 4c_4^2 \ge \int_{t_0}^{\infty} |\nu|^2 d\tau.$$

Hence, from (31), it follows that

$$V(t) - V(t_0) < 0 \qquad \forall \quad t \ge t_1. \tag{32}$$

Also, over $[t_0, t_1]$, since $\int_{t_0}^{t_1} \|e\|^2 d\tau < 4c_4^2$,

$$V(t) \le V(t_0) + 8c_2 c_4^2 = c_6 \qquad \forall \quad t \in [t_0, t_1]. \tag{33}$$

Equations (32) and (33) imply that $V(t)$, and hence, $e(t)$ and $\phi(t)$ are bounded for all $t \ge t_0$. We now show that $e \in \mathcal{L}^2$ by contradiction. Let $e \notin \mathcal{L}^2$. This implies that

$$\int_{t_0}^{t} \|e(\tau)\|^2 d\tau \to \infty \qquad \text{as} \quad t \to \infty.$$

Equation (31) can therefore be simplified as

$$V(t) \le V(t_0) - c_7 \int_{t_0}^{t} \|e(\tau)\|^2 d\tau \le -c_8 < 0 \qquad \text{for some finite } t. \tag{34}$$

This contradicts the choice of $V(t)$ which is positive for all $t \ge t_0$. Therefore $e \in \mathcal{L}^2$. Finally, when $\omega(t)$ and $\nu(t)$ are also bounded, it follows that $\dot{e} \in \mathcal{L}^\infty$. Since $e \in \mathcal{L}^2 \cap \mathcal{L}^\infty$ and $\dot{e} \in \mathcal{L}^\infty$, we obtain as in the disturbance-free case that

$$\lim_{t\to\infty} e(t) = 0.$$

REFERENCES

[1] Balas, M. J. (1982)
Trends in large space structure control theory: Fondest hopes, wildest dreams.
IEEE Transactions on Automatic Control, **AC-27** (1982), 522–535.

[2] Meirovitch, L., Baruh, H., and Oz, H. (1983)
A comparison of control techniques for large flexible systems.
Journal of Guidance, Control and Dynamics, **6** (1983), 514–526.

[3] Joshi, S. M. (1989)
Control of Large Flexible Space Structures.
New York: Springer-Verlag, 1989.

[4] Joshi, S. M., and Maghami, P. G. (1992)
Robust dissipative compensators for flexible spacecraft control.
IEEE Transactions on Aerospace and Electronic Systems, **28** (1992), 768–774.

[5] Benhabib, R. J., Iwens, R. P., and Jackson, R. L. (1981)
Stability of large space structure control systems using positivity concepts.
Journal of Guidance, Control and Dynamics, **4** (1981), 487–494.

[6] Narendra, K. S., and Annaswamy, A. M. (1989)
Stable Adaptive Systems.
Englewood Cliffs, NJ: Prentice Hall, 1989.

[7] Morse, A. S. (1985)
A three-dimensional universal controller for the adaptive stabilization of any strictly proper minimum phase system with relative degree not exceeding two.
IEEE Transactions on Automatic Control, **AC-30** (1985), 1188–1191.

[8] Mudgett, D. R., and Morse, A. S. (1985)
Adaptive stabilization of linear systems with unknown high frequency gains.
IEEE Transactions on Automatic Control, **AC-30** (June 1985), 549–554.

[9] Bar-Kana, I., Kaufman, H., and Balas, M. J. (1983)
Model reference adaptive control of large structural systems.
Journal of Guidance, Control and Dynamics, **6** (1983), 112–118.

[10] Ih, C. C., Wang, S. J., and Leondes, C. T. (1985)
An investigation of adaptive control techniques for space stations.
In *Proceedings of the ACC*, San Francisco, CA, 1985, 81–94.

[11] Bayard, D. S., Ih, C. C., and Wang, S. J. (1987)
Adaptive control for flexible space structures with measurement noise.
In *Proceedings of the ACC*, San Francisco, CA, 1987, 368–379.

[12] O'Brien, M., and Broussard, J. R. (1978)
Feedforward control to track the output of a forced model.
In *Proceedings of the 17th CDC*, San Francisco, CA, 1978, 1149–1154.

[13] Davison, E. J. (1976)
The steady-state invertibility and feedforward control of linear time-invariant systems.
IEEE Transactions on Automatic Control, **AC-21** (1976), 529–534.

[14] Sobel, K., Kaufman, H., and Mabius, L. (1982)
Implicit adaptive control for a class of mimo systems.
IEEE Transactions on Aerospace and Electronic Systems, **AES-18** (1982), 576–590.

[15] Carrier, A., and Aubrun, J-N. (1992)
Modal characterization of the ascie segmented optics test bed: New algorithms and experimental results.
In *Proceedings of the AIAA Guidance and Control Conference*, Hilton Head, SC, 1992.

[16] Vivian, H. C., Blaire, P. E., Eldred, D. E., Fleischer, G. E., Ih, C. C., Nerheim, N. M., Schied, R. E., and Wen, J. T. (1987)
Flexible structure control laboratory development and technology demonstration.
Technical report final report, JPL Publication 88-29, 1987.

[17] Delorenzo, M. L. (1990)
Sensor and actuator selection for large space structure control.
Journal of Guidance, Control and Dynamics, **13** (1990), 249–257.

[18] Fanson, J. L., and Caughey, T. K. (1987)
Positive position feedback control for large space structures.
In *Proceedings of the 28th AIAA Structures, Structural Dynamics, and Materials Conference*, San Francisco, CA, 1987, 588–590.

[19] Crawley, E. F., and de Luis, J. (1987)
Use of piezoelectric actuators as elements of intelligent structures.
AIAA Journal, **25** (1987), 1373–1385.

[20] Eldred, D., and Schaechter, D. (1981)
Experimental demonstration of static shape control.
In *Proceedings of the AIAA Guidance and Control Conference*, Albuquerque, NM, 1981.

[21] Mufti, I. H. (1987)
Model reference adaptive control for large structural systems.
Journal of Guidance, Control and Dynamics, **5** (1987), 507–509.

[22] Ioannou, P. A., and Kokotovic, P. V. (1983)
Adaptive Systems with Reduced Models.
New York: Springer-Verlag, 1983.

[23] Narendra, K. S., and Annaswamy, A. M. (1987)
A new adaptive law for robust adaptive control without persistent excitation.
IEEE Transactions on Automatic Control, **32** (Feb. 1987).

[24] Narendra, K. S., and Valavani, L. S. (1978)
Stable adaptive controller design-direct control.
IEEE Transactions on Automatic Control, **23** (Aug. 1978), 570–583.

[25] Zeheb, E. (1986)
A sufficient condition for output feedback stabilization of uncertain systems.
IEEE Transactions on Automatic Control, **AC-31** (1986).

[26] Annaswamy, A. M. (1992)
A new adaptive controller.
In *Proceedings of the 1992 American Control Conference*, Chicago, IL, 1992.

[27] Hughes, P. C., and Skelton, R. E. (1980)
Controllability and observability for flexible spacecraft.
Journal of Guidance, Control and Dynamics, **5** (1980), 452–459.

[28] Bakker, R., and Annaswamy, A. M. (1994)
Simple multivariable adaptive control with application to flexible structure.
In *Proceedings of the ACC*, Baltimore, MD, 1994.

Anuradha Annaswamy (S'82—M'85) received the B.S. degree in mathematics from Madras University, Madras, India, in 1976, the B.E. degree in electrical engineering from Indian Institute of Science in 1979, and the M.S. and Ph.D. degrees in electrical engineering from Yale University, New Haven, CT, in 1980 and 1985, respectively.

She was a post-doctoral fellow from 1985–1987 and subsequently a visiting Assistant Professor at Yale. During 1988–1991, she was at Boston University in the Department of Aerospace and Mechanical Engineering as an Assistant Professor. Currently, she is with the Department of Mechanical Engineering at MIT as an Associate Professor. Dr. Annaswamy's research interests are in the control of complex dynamical systems in the presence of uncertainties with applications to flexible structures, high performance aircraft, and combustion systems. She has published several articles in conferences and journals, as well as a graduate-level textbook, *Stable Adaptive Systems* (co-author: K. S. Narendra) in the areas of adaptive control theory and applications.

Dr. Annaswamy has received a number of awards and honors including the Alfred Hay Medal from the Indian Institute of Science in 1977, the Arthur E. Stennard Fellowship from Yale University in 1980, the IBM post doctoral fellowship from 1985–1986, the George Axelby Outstanding Paper award from IEEE Control Systems Society in 1988, and the Presidential Young Investigator award from the National Science Foundation in 1991. She is a member of AIAA and Sigma Xi.

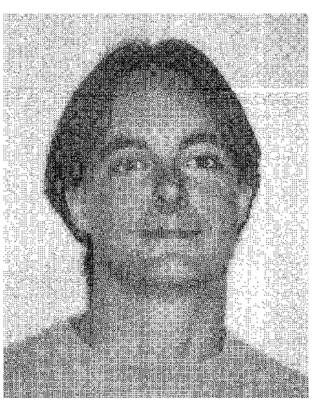

Daniel J. Clancy received the M.S. degree in electrical engineering from Boston University, Boston, MA, in 1991. He is currently a Ph.D. student in electrical engineering at The Ohio State University.

From 1988–1992, he worked as a control engineer in the Systems Design Laboratory at Raytheon Company, Tewksbury, MA. His research interests include artificial neural networks, wavelets, robust multivariable control, and adaptive control with application to flexible structures.